

Anisotropy of ultra-high-energy cosmic rays in the single-source diffusion model

V. S. Berezinskiĭ, S. I. Grigor'eva, and V. A. Dogel'

P. N. Lebedev Institute of Physics, Academy of Sciences of the USSR

(Submitted 7 April 1989)

Zh. Eksp. Teor. Fiz. **96**, 798–810 (September 1989)

The anisotropy of ultra-high-energy ($E > 10^{18}$ eV) cosmic rays is studied in the single-pulsed-source diffusion model. It is shown that for short duration of the production pulse ("instantaneous source") the anisotropy decreases with increasing energy. The increase in anisotropy with energy for longer duration is not as significant as in stationary diffusion models. A model of the origin of the ultra-high-energy ($E > 10^{18}$ – 10^{19} eV) cosmic rays is considered where they are generated in a nearby active galactic nucleus (NGC 4151 or Cen A). The spectra and their anisotropies are calculated in these models. The anisotropy may be at most 10–20% for $E \sim 10^{19}$ eV.

1. INTRODUCTION

At the present time it is generally accepted^{1–3} (see also the reviews in Refs. 4 and 5) that the end of the cosmic ray (CR) spectrum is of extra-galactic origin. Three types of extra-galactic models are discussed in the literature: 1) metagalactic model with⁶ and without⁷ evolution of the sources taken into account; 2) a local supercluster model¹ on the assumption of many sources, and 3) a single-source model,² whose role is played by the Virgo galactic cluster in the Local supercluster.

The present work is devoted to the single-source model. Interest in this model is due, in part, to the fact that it is possible here to form the spectrum without the blackbody cutoff. Let us imagine that the source of ultra-high-energy (CR) consists of only very powerful rare sources (for example, quasars of a definite type or very powerful Seyfert galaxies). For an observer close to such a source, the spectrum of the CR will be determined in the main by the source, and owing to the short propagation time of the particles the blackbody cutoff of the spectrum will be shifted to higher energies or be altogether absent. It may be that this situation occurs in reality because of the accidental proximity of our Galaxy to the powerful Seyfert type I galaxy NGC 4151 ($r = 13.2$ Mpc for a Hubble constant $H_0 = 75$ km/sec·Mpc, which we shall use throughout). However this is not the only possibility. The source could be a nearby "extinguished" galaxy, the activity of whose nucleus ended 10^8 – 10^9 years ago, and the cosmic rays reach us only now due to the long propagation time. In such a case it is hard to indicate a concrete galaxy as the source.

From estimates of the duration τ_{AGN} and the calculated propagation time for the cosmic rays, $\tau_{\text{cr}} \lesssim 10^9$ years, for distances $r \leq 10$ – 20 Mpc the model of a source with an active nucleus, that would be currently observable, seems preferred. Indeed, if one supposes that the energetics of the galactic nucleus is ensured by gas accretion by a massive black hole, then for powerful sources with luminosity of the order of Eddington luminosity $L_{\text{Edd}} = 1.3 \cdot 10^{38} M_h/M_\odot$ erg/sec, the duration of the active phase amounts to $\tau_{\text{AGN}} \sim M_g/L_{\text{Edd}}$, where M_h is the mass of the black hole, M_g is the mass of the accreted gas, and M_\odot is the mass of the Sun. Under the natural assumption that $M_g \sim M_h$ we obtain $\tau_{\text{AGN}} \approx 4 \cdot 10^8$ years. For a source with $L < L_{\text{Edd}}$ this time is even larger.

This paper is devoted to a phenomenological study of the spectra and the anisotropy of ultra-high energy cosmic

rays in the single-source model. We shall make use of the generally accepted concept, that the particles may be accelerated to ultra-high energies in active galactic nuclei (see Refs. 8–12, and also the reviews in Refs. 4, 5 and the literature cited therein) and will suppose that the particle production spectrum is given by a power law in the entire energy interval from $E_{\text{min}} \sim 1$ GeV up to the highest observed energies, and the luminosity in the accelerated particles equals L_p . The neutron mechanism for the particles' escape from the galactic nucleus¹³ results in a pure proton content of the cosmic rays emitted by the source. It should be noted that the acceleration of the particles in active galactic nuclei is an unsolved problem. The presence of high electric potential in the accretion disk^{8,9} does not yet mean acceleration of the particles to corresponding energies. The electrodynamics of the accretion disk is analogous to the electrodynamics of a pulsar with free discharge. The acceleration is related to the component E_{\parallel} of the electric field along the direction of the magnetic field. The free discharge models are too poorly developed to provide quantitative predictions for the maximal acceleration energy.

Acceleration by shock wave fronts in active galactic nuclei^{10–12} is, apparently, limited by photopion energy losses.¹⁴

This article is organized as follows. In Sec. 2 we discuss the possibility of diffusion propagation of ultra-high energy particles in the Local galactic supercluster. In Sec. 3 we obtain general restrictions on the diffusion coefficient. In Sec. 4 we give general formulas for the spectra and anisotropy. In Sec. 5 we find an analytic solution for the anisotropy in the case of "instantaneous source" (duration of the production pulse T much less than the propagation time). In Sec. 6 we give results of numerical calculations of spectra and anisotropy and give their interpretation. A comparison with observations is made. In the Conclusion we formulate the main results.

2. ON THE POSSIBILITY OF DIFFUSION PROPAGATION OF PARTICLES IN THE LOCAL SUPERCLUSTER

Diffusion propagation of ultra-high energy protons in the Local galactic supercluster was studied in Ref. 15. In that paper a study was made of the problem of particle scattering by magnetic clouds of linear dimension l and regular field \mathbf{H} on the assumption of a small mean scattering angle of the particle by the cloud $\bar{\theta} \sim l/r_H < 1$ (where r_H is the Lar-

mor radius of the particle). At a distance from the source $r < r_0$, where

$$r_0 = 16l/3\theta^2, \quad (1)$$

the particles propagate practically in straight lines and the angular distribution of the particles, observed a time t after emission, is described by the Gauss law

$$n(t, \theta) = At^{-1/2} \exp(-l\theta^2/2ct\theta^2).$$

The probability of finding a proton at a distance $r \gg r_0$ from the source is equal to the probability of translation of the particle from the equilibrium location as a result of fluctuations, described by the Gaussian distribution

$$\bar{r} = (32/3\pi^2) (clt/\theta^2)^{1/2}.$$

In this fashion propagation for $r \gg r_0$ has the diffusion character with diffusion coefficient given by

$$D(E) = (32/3\pi^2)^2 cl/6\theta^2 \propto E^2. \quad (2)$$

For cloud parameters assumed in Ref. 15, $l \sim 0.1$ Mpc and $H \sim 10^{-8}$ G, the protons propagate in the Supercluster ($r \approx 20$ Mpc) practically rectilinearly, beginning with an energy of $E \sim 1 \cdot 10^{19}$ eV, which contradicts the single-source model. In the diffusion model² the same cloud parameters are used ($l \approx 0.1$ Mpc, $H \sim 10^{-8}$ G, but a different energy dependence of the diffusion coefficient is assumed, $D(E) \propto E^1$, which may be due to a distribution of the clouds in the quantity lH).

In the cited papers, the parameters of the magnetic field in the Local supercluster were chosen arbitrarily. The structure of the magnetic field may be primary or produced in a specific manner in the Local supercluster. We wish to discuss the possibility of producing the structure of a quasiregular field by the galactic wind. This mechanism was discussed in Ref. 16 for the production of the large-scale field in the halo of our Galaxy. It is assumed in the galactic-wind picture that a hot gas with "frozen in" magnetic field escapes from the galaxy with a velocity in excess of parabolic $v_c \approx 3 \cdot 10^7$ cm/sec. Although the appearance of the wind has been discussed in several papers (see, for example, Refs. 17, 18), this phenomenon cannot be viewed as proven and in fact an alternative process is possible: accretion of metagalactic gas by the galaxy.^{19,20}

For further estimates we assume parameters for the galactic wind used in Ref. 16: luminosity $L_w = 5 \cdot 10^{40}$ erg/sec of the galaxy in the form of the galactic wind and velocity $v_w \approx 1 \cdot 10^8$ cm/sec. The galactic wind fills around the galaxy a bubble of radius equal to half the average distance R between galaxies in the Local supercluster. For a spatial density²¹ of galaxies in the supercluster of $n_g \approx 1 \cdot 10^{-75}$ cm⁻³ we have $R \sim 1$ Mpc. The wind energy density in the bubble is

$$\omega_w \sim L_w n_g T_{LS} \approx 2 \cdot 10^{-17} \text{ erg/cm}^3,$$

where $T_{LS} \approx 1 \cdot 10^{10}$ years is the age of the Local supercluster.

The bubble is filled with a regular magnetic field, exported from the galaxy by the wind. Let us find it from the equipartition condition

$$H \propto (8\pi\omega_w)^{1/2} \approx 2 \cdot 10^{-8} \text{ G}. \quad (3)$$

It is easy to convince oneself that a bubble with these parameters has the negligibly small measure of Faraday rotation

$\sim 10^{-4}$ rad/m² and cannot, therefore, be detected in polarization experiments. The energy of a proton trapped in the bubble equals

$$E_s \sim eHR \approx 2 \cdot 10^{19} \text{ eV},$$

and the maximum energy, for which the diffusion approximation is valid, is larger than E_s , as a result of scattering on various bubbles. The Bohm diffusion coefficient is

$$D(E) \approx 1/3 r_H c \approx 2 \cdot 10^{34} (E/10^{19} \text{ eV}) \text{ cm}^2/\text{sec}.$$

The estimates given above are, of course, quite rough; in particular they refer to average quantities only. In the calculations that follow we shall make use of the phenomenological expression for the diffusion coefficient

$$D(E) = D_0 (E/10^{19} \text{ eV})^\beta \quad (4)$$

with $D_0 \approx (1-5) \cdot 10^{34}$ cm²/sec and $\beta \approx 0.5-0.8$. In practice the assumption on the size of D_0 is more critical here, since particles with $E < 1 \cdot 10^{19}$ eV have, most likely, galactic origins, and in the interval $10^{19}-10^{20}$ eV of interest a change in β from 0.5 to 1 (or from 0.8 to 1) has no significant effect on the results presented below.

3. GENERAL RESTRICTIONS ON THE DIFFUSION COEFFICIENT AT ULTRA-HIGH ENERGIES

We consider first a stationary single source. An upper bound on the diffusion coefficient follows from the requirement that the diffusion propagation time $t_d \approx r^2/6D$ should be larger than the time for direct flight $t = r/c$:

$$D_{\max} < 1/6 rc. \quad (5)$$

In particular for NGC 4151 we have $D_{\max} < 2 \cdot 10^{35}$ cm²/sec. Let us note that $D(E) = 3 \cdot 10^{35} (E/10^{19} \text{ eV})^1$ cm²/sec, which is the diffusion coefficient used in Ref. 2, exceeds D_{\max} for an energy $E \geq 1 \cdot 10^{19}$ eV.

On the other hand, $E \gtrsim 5 \cdot 10^{19}$ eV, when photopion reactions become significant, a lower bound on the diffusion coefficient results. It is due to neutron production in collisions with relict photons. The nucleon diffusion path length l_d is longer in this case than the neutron decay path length $c\tau_n E/m_n c^2$, where τ_n is the neutron lifetime and m_n is its mass (we ignore the contribution of the proton to the diffusion path length). This means that the diffusion coefficient must satisfy the condition

$$D(E) > \tau_n E/3m_n = 1.5 \cdot 10^{34} (E/5 \cdot 10^{19} \text{ eV}) \text{ cm}^2/\text{sec}. \quad (6)$$

Let us note that the bounds, Eqs. (5) and (6), have the character of strong inequalities; for Eq. (6) this is due, in part, to the fact that the energy is higher at the instant of production than of observation. A comparison of these bounds shows that for a stationary source at a distance $r \sim 10-20$ Mpc for an energy $E \sim (0.5-1) \cdot 10^{20}$ eV diffusion propagation should be replaced by quasirectilinear propagation, and the anisotropy should drastically increase.

For a nonstationary source, which injects particles in the form of a short pulse of duration $T \ll t$, where t is the time interval between the turning on of the source and the observation, the restriction, Eq. (5), is formally removed. The diffusion coefficient $D(E)$ may exceed D_{\max} , and this means that at some instant of time prior to observation a large direct stream of particles with energy higher than E passed

through the observation point. At the instant of observation t , on the other hand, the stream of particles with this energy is suppressed by a factor $t^{-3/2}$ or even stronger, if the particles suffered an energy loss.

4. SPECTRUM AND ANISOTROPY (GENERAL FORMULAS)

We consider a source at a distance r from the observer, emitting protons in the form of pulses of duration T . We suppose that the differential production spectrum has the form

$$Q(E_g) = K(E_g + \bar{E}_m)^{-(\gamma+1)}, \quad (7)$$

where E_g is the kinetic energy of the proton, $\bar{E}_m \sim 1$ GeV is a normalization energy, γ is the production exponent, and the constant K is expressed in terms of the luminosity of the source in accelerated protons:

$$K = \gamma(\gamma-1) L_p \bar{E}_m^{\gamma-1}. \quad (8)$$

The equation for the density of particles $n(\mathbf{r}, E, t)$ in the space around the source has the form²²

$$\frac{\partial n}{\partial t} - D(E) \nabla^2 n + \frac{\partial}{\partial E} [b(E)n] = Q(E_g) \delta(\mathbf{r}_g) \theta(t_g) \theta(T-t_g), \quad (9)$$

where r_g is the distance from the production point, t_g is the production instant, and $b(E) = -dE/dt$ describes the energy losses of the protons during propagation; at the ultra-high energies considered here the losses are determined by the interaction with relict radiation:

$$p + \gamma_{\text{rel}} \rightarrow p + e^+ + e^-, \quad p + \gamma_{\text{rel}} \rightarrow \pi + X.$$

The energy losses calculated by us are given in Ref. 23. We search for a solution of Eq. (9) by the Syrovatskii method,²⁴ by going over to the variables

$$\tau(E, E_g) = \int_E^{E_g} \frac{dE'}{b(E')}, \quad (10)$$

$$\lambda(E, E_g) = \int_E^{E_g} \frac{D(E') dE'}{b(E')}. \quad (11)$$

Here the Green function is

$$f(\mathbf{r}, E, t, \mathbf{r}_g, E_g, t_g) = \frac{1}{b(E)} \frac{\exp[-(\mathbf{r}-\mathbf{r}_g)^2/4\lambda]}{(4\pi\lambda)^{3/2}} \delta(t-t_g-\tau),$$

and the solution of Eq. (9) is

$$n(\mathbf{r}, E, t) = \int_0^\infty dE_g \frac{K E_g^{-(\gamma+1)}}{b(E)} \frac{\exp[-r^2/4\lambda(E, E_g)]}{[4\pi\lambda(E, E_g)]^{3/2}} \times \theta(t-\tau) \theta(T-t+\tau).$$

Replacing the θ -functions by the limits on the integration over E_g , we obtain finally for the density of protons with energy E at a distance r at the instant of observation t , assuming that the source was turned on at time zero:

$$n(E, \mathbf{r}, t) = K \frac{1}{b(E)} \int_{\xi(E, t-T)E}^{\xi(E, t)E} dE_g E_g^{-(\gamma+1)} \frac{\exp[-r^2/4\lambda(E, E_g)]}{[4\pi\lambda(E, E_g)]^{3/2}}, \quad (12)$$

where the function $\xi(E, t)$ connects the proton energy E at the instant of observation to the proton energy E_g at the instant of production $t_g = 0$:

$$E_g = \xi(E, t) E. \quad (13)$$

The function $\xi(E, t)$ is found by numerical integration of the equation $dE/dt = -b(E)$.

The anisotropy is calculated from the expression

$$\delta(E) = \frac{3}{c} \frac{D(E)}{n(E, \mathbf{r}, t)} \left| \frac{\partial n(E, \mathbf{r}, t)}{\partial r} \right|, \quad (14)$$

where

$$\left| \frac{\partial n(E, \mathbf{r}, t)}{\partial r} \right| = 2\pi K \frac{r}{b(E)} \int_{\xi(E, t-T)E}^{\xi(E, t)E} dE_g E_g^{-(\gamma+1)} \frac{\exp[-r^2/4\lambda(E, E_g)]}{[4\pi\lambda(E, E_g)]^{3/2}}. \quad (15)$$

Before going to numerical results we make two general remarks.

1. The function, Eq. (12), makes it possible to find the current density $j(E, \mathbf{r}, t) = (c/4\pi)n(E, \mathbf{r}, t)$ as a function of the distance from the source \mathbf{r} , the maximal propagation time¹⁾ t and the energy E . In a previous paper^{2,3} we have calculated the spectrum of a single source for fixed time of propagation. The characteristic feature of the spectrum is the blackbody cutoff and the hump due to slowed-down particles. The spectrum, Eq. (12), differs from the spectra of Ref. 23 by a distribution of various times of propagation. Naturally, the spectra of Eq. (12) look qualitatively the same as those in Ref. 23. The spectra also coincide quantitatively in the case of the instantaneous source.

2. In our problem the instant of turning on the source (taken as zero) and the moment of observation t are fixed. Even for $T > t$ this problem does not reduce to stationary diffusion, and this is why one gets the unusual dependence of the anisotropy on energy.

5. ANISOTROPY IN THE CASE OF INSTANTANEOUS SOURCE

There exists the widely disseminated dogma that if the diffusion coefficient increases with energy, then so does the anisotropy. In our problem this is not so and, in particular, the anisotropy may decrease with increasing energy. To obtain an understanding of the physics of this phenomenon we consider here the analytically soluble case of the instantaneous ($T \ll t$) source.

The instantaneous source is characterized by the fact that t becomes the propagation time and the production energy becomes a function of E and t only. For $T \ll t$ the integrand in Eqs. (12) and (15) changes little; one power of $\lambda(E, E_g)$ in the denominator in Eq. (15) may be taken outside the integral and then we obtain from Eq. (14)

$$\delta(E) = \frac{3D(E)}{2c} \frac{r}{\lambda(E, t)}. \quad (16)$$

If $D(E) = D_0$, then it follows from Eq. (11) that

$$\lambda(E, t) = D_0 \tau(E, E_g) = D_0 t$$

and from Eq. (16) we obtain the familiar expression

$$\delta \approx \delta_0 = 3r/2ct \quad (17)$$

Let us consider now the case $D(E) = D_0 E^\beta$ and $|dE/dt| = b(E) = E/\tau_0$, where τ_0 is the characteristic slowing-down time. Then we integrate Eq. (11) to obtain $\lambda(E, t)$, which when substituted into Eq. (16) gives

$$\delta = \delta_0 x / (e^x - 1), \quad (18)$$

where $x = \beta t / \tau_0$.

For a nearby source ($t \ll \tau_0/\beta$) we have $\delta \approx \delta_0$, for a distant source ($t \gg \tau_0/\beta$) we have $\delta \approx \delta_0 x e^{-x} < \delta_0$. For realistic energy losses (see Ref. 23 and the scheme in Fig. 1) $b(E)/E = \tau_{01} = B_0^{-1}$ at low energies and $b(E)/E = \tau_{02} = B_1^{-1}$ at high energies, and $\tau_{02} \ll \tau_{01}$. In other words, at low energies the source is nearby ($\delta \approx \delta_0$), while at high energies the source is distant ($\delta \approx \delta_0 x e^{-x} < \delta_0$), i.e., the anisotropy decreases with energy.

For a physical interpretation we turn to formula (16) and rewrite it in the form $\delta(E) = \delta_0 D(E)t / \lambda(E, t)$. The numerator $D(E)t$ is the square of the distance traveled by the particle in time t under the condition of constancy of its energy. The quantity

$$\lambda(E, t) = \int_E^{E_g(E, t)} D(E') \frac{dE'}{dE'/dt} = \int_0^t D(E') dt$$

has the meaning of the square of the distance traveled in time t with the change in the particle energy taken into account. At low energies, when the change in the energy is insignificant, i.e. $(E^{-1} dE/dt)t \ll 1$, we have

$$\lambda(E, t) = D(E)t, \quad \delta \approx \delta_0.$$

At high energies, when the energy losses are significant, we have

$$D(E') > D(E), \quad \lambda(E, t) > D(E)t$$

and the anisotropy $\delta < \delta_0$.

We give the analytic solution for anisotropy in the case $D(E) = D_0 E^\beta$ and for a very close to realistic description of energy losses (see Fig. 1):

$$\frac{1}{E} \frac{dE}{dt} = \begin{cases} B_0, & E < E_0, \\ B_0 (E/E_0)^\alpha, & E_0 < E < E_1, \\ B_1, & E > E_1. \end{cases}$$

We consider the realistic case $B_1^{-1} < t < B_0^{-1}$, when the cutoff energy E_c , determined in Fig. 1 by the point of intersec-

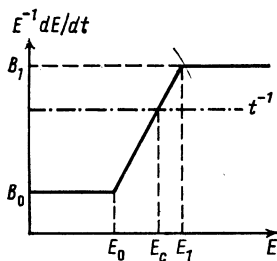


FIG. 1. Dependence of the energy losses $E^{-1}dE/dt = -b(E)/E$ on the energy E : t —propagation time, E_c —cutoff energy.

tion of the straight line t^{-1} with the losses curve, is less than E_1 .

Since the integral in Eq. (11) can be evaluated analytically and $\delta(E)$ is calculated according to Eq. (16), the problem reduces to the calculation of the production energy, with the energy losses indicated above taken into account. As a result of simple calculations we obtain the following expressions for the production energy and the anisotropy: for $E < E_0 \exp(-B_0 t)$

$$E_g(E, t) = E \exp(B_0 t), \quad \delta \approx \delta_0, \quad (19)$$

for $E_0 < E < E_1(1 + \alpha B_1 t)^{-1/\alpha}$

$$E_g(E, t) = E [1 - \alpha B_0 t (E/E_0)^\alpha]^{-1/\alpha}, \quad (20)$$

$$\delta(E) = \delta_0 (\alpha - \beta) B_0 t [1 - (E_g/E)^{-(\alpha-\beta)}]^{-1} (E/E_0)^\alpha$$

for $E_1(1 + \alpha B_1 t)^{-1/\alpha} \leq E < E_1$

$$\begin{aligned} E_g(E, t) &= E [1 - \alpha B_0 t (E/E_0)^\alpha]^{-1/\alpha}, & t \leq t_1, \\ E_g(E, t) &= E_1 \exp[B_1(t - t_1)], & t \geq t_1, \end{aligned} \quad (21)$$

$$\begin{aligned} \delta &= \delta_0 \beta B_0 t \left(\frac{E}{E_0} \right)^\beta \left(\frac{E_1}{E_0} \right)^{\alpha-\beta} \left\{ \exp[\beta B_1(t - t_1)] \right. \\ &\quad \left. - 1 + \frac{\beta}{\alpha - \beta} \left(\frac{E}{E_1} \right)^{-(\alpha-\beta)} - \frac{\beta}{\alpha - \beta} \right\}^{-1}, \end{aligned}$$

where t_1 is determined by the equation $E_g(E, t_1) = E_1$, and, lastly, for $E > E_1$

$$E_g(E, t) = E \exp(B_1 t), \quad \delta = \delta_0 \tilde{x} [\exp(\tilde{x}) - 1]^{-1}, \quad (22)$$

where $\tilde{x} = \beta B_1 t$. The energy dependence of the anisotropy, determined by Eqs. (19)–(22), is shown schematically in Fig. 2.

6. SPECTRA AND ANISOTROPY (NUMERICAL CALCULATIONS)

Here we give results of numerical calculations of the spectra and anisotropy according to Eqs. (12), (14) and (15), where the quantity K is related to the luminosity of the source by Eq. (8). The diffusion coefficient will be taken as

$$D(E) = D_0 (E/10^{19} \text{ eV})^\beta. \quad (23)$$

The model is defined by the choice of source (the distance r from it, the luminosity in the accelerated protons L_p) and the parameters that characterize the propagation: the time t from the turning on of the source to the instant of observation (maximal propagation time), duration of the produc-

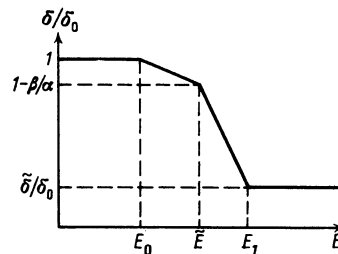


FIG. 2. Energy dependence of the anisotropy for the instantaneous-source model calculated according to Eqs. (19)–(22). $\delta/\delta_0 = \tilde{x} [\exp(\tilde{x}) - 1]^{-1}$ and $\tilde{E} = E_1(1 + \alpha B_1 t)^{-1/\alpha}$.

tion pulse T , the quantities D_0 and β . Formally we give solutions up to energies 10^{20} – 10^{21} eV, but in fact the maximal energy for which the diffusion approximation is valid is restricted in accordance with the considerations in Sec. 3.

As an example we give the calculation of the spectrum and anisotropy for a model where the source was taken to be the Seyfert galaxy NGC 4151 ($r = 13.2$ Mpc). The calculated spectra and anisotropy are shown in Fig. 3 for a luminosity of the source in accelerated protons $L_p = 1 \cdot 10^{44}$ erg/sec (the observed luminosity of the source amounts to $L \sim 10^{45}$ erg/sec) and time between turning on of the source and observation $t = 3 \cdot 10^8$ years. The remaining parameters of the model are indicated in the caption of Fig. 3.

The energy spectra of Fig. 3 are characterized by a late blackbody cutoff $E_c \approx 8 \cdot 10^{19}$ eV, and a hump preceding the cutoff. Naturally, with increased duration of the production pulse the current increases.

For short duration of the production pulse $T \leq 1 \cdot 10^7$ years the anisotropy is described by the universal curve 1 (Fig. 3). It corresponds precisely to the Eqs. (19)–(22) for an instantaneous source, obtained in the preceding section. A change in the character of the dependence $\delta(E)$ with increasing T may be understood qualitatively by considering the anisotropy as $T \rightarrow t$:

$$\delta(E) = \frac{3D(E)r}{2c} \int_E^{E_g(E,t)} \frac{1}{\lambda} dE_g'(E_g')^{-(\tau+1)} (4\pi\lambda)^{-\eta} \exp(-r^2/4\lambda) \times \left[\int_E^{E_g(E,t)} dE_g'(E_g')^{-(\tau+1)} (4\pi\lambda)^{-\eta} \exp\left(-\frac{r^2}{4\lambda}\right) \right]^{-1} = \frac{3D(E)r}{2c} \langle \lambda^{-1} \rangle. \quad (24)$$

The integrand in Eq. (24) has a maximum for $E_g' = E_m$, where $\lambda(E, E_m) \sim r^2$. For small E , when E_g differs little from E , this maximum lies outside the limits of integration and, as is easily understood, the quantity $\langle \lambda^{-1} \rangle$ may be estimated as λ^{-1} taken at the upper integration limit. One obtains in this way $\langle \lambda^{-1} \rangle = 1/D(E)t$ and $\delta(E) \approx 3r/2ct \equiv \delta_0$ in accordance with numerical calculations. At high energies the limits of integration are moved apart by the energy losses and the maximum falls inside the limits of integration. In that case $\lambda^{-1}(E, E_g')$ should be taken outside the integral at the maximum point $E_g' = E_m$, where $\lambda(E, E_m) \sim r^2$. This gives an anisotropy $\delta(E) \approx 3D(E)/2cr$ that increases with energy like E^β . A gradual transition to this regime can be seen in Fig. 3.

Against the background of increasing anisotropy a distinctive dip can be seen in the curves in Fig. 3, corresponding to the energy at which the photopion hump appears in the spectrum. This dip is explained by the fact that the hump is due to protons slowed down from higher energies. As a result the quantity

$$\lambda(E, t) = \int_E^{E_g(E,t)} D(E_g') \frac{dE_g'}{dE_g'/dt} = \int_0^{\tau(E, E_g)} D(E_g') dt$$

increases in a jump as E falls into the region of the hump, and, according to Eq. (24), this gives a drastic reduction in anisotropy.

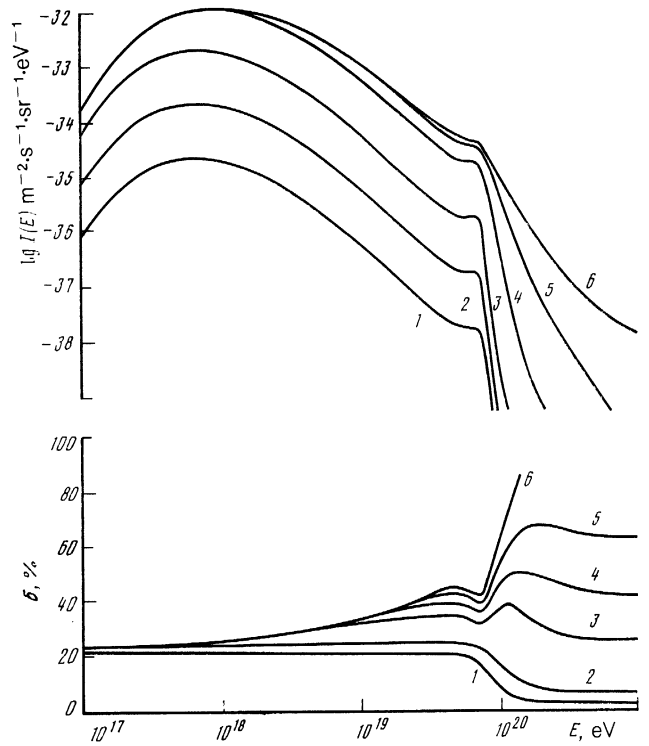


FIG. 3. The spectra and anisotropy in the model with NGC 4151 ($r = 13.2$ Mpc) as source for $t = 3 \cdot 10^8$ years, $\gamma = 1.1$, $L_p = 1 \cdot 10^{44}$ erg/sec, $D_0 = 3 \cdot 10^{34}$ cm²/sec and $\beta = 0.5$. The spectral curves are labeled by the duration of the production pulse T : 1— $1 \cdot 10^5$ years; 2— $1 \cdot 10^6$ years; 3— $1 \cdot 10^7$ years; 4— $1 \cdot 10^8$ years; 5— $2 \cdot 10^8$ years; 6— $3 \cdot 10^8$ years. The anisotropy curves are labeled according to: 1— $T \leq 1 \cdot 10^7$ years; 2— $1 \cdot 10^8$ years; 3— $2 \cdot 10^8$ years; 4— $2.3 \cdot 10^8$ years; 5— $2.5 \cdot 10^8$ years; 6— $3 \cdot 10^8$ years.

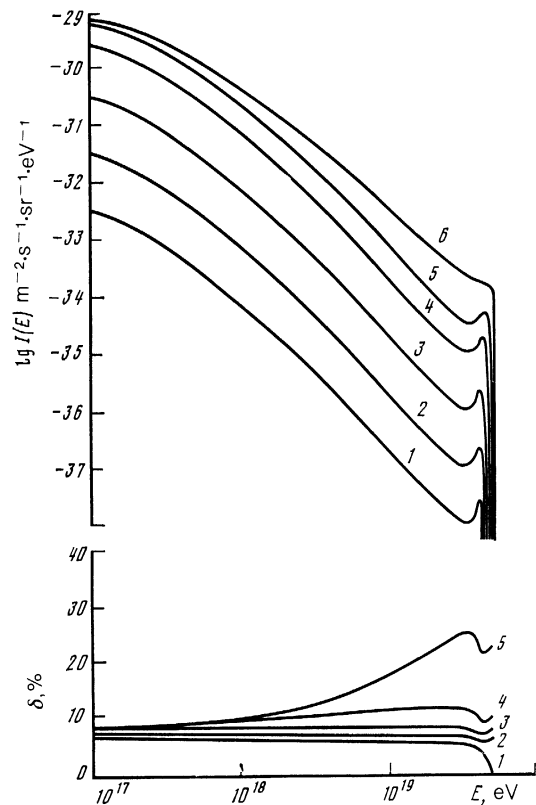


FIG. 4. Same as Fig. 3 for $t = 1 \cdot 10^9$ years. The spectral curves correspond to: 1— $T = 1 \cdot 10^5$ years; 2— $1 \cdot 10^6$ years; 3— $1 \cdot 10^7$ years; 4— $1 \cdot 10^8$ years; 5— $3 \cdot 10^8$ years; 6— $1 \cdot 10^9$ years. The anisotropy curves: 1— $T \leq 1 \cdot 10^7$ years; 2— $3 \cdot 10^8$ years; 3— $5 \cdot 10^8$ years; 4— $7 \cdot 10^8$ years; 5— $1 \cdot 10^9$ years.

As the maximal propagation time increases to $t = 1 \cdot 10^9$ years (Fig. 4) the following changes take place: a) the black-body cutoff energy of the spectrum is shifted to lower values ($E_c \approx 5 \cdot 10^{19}$ eV) resulting in the hump becoming more prominent; b) the cutoff of the spectrum becomes sharper; c) the anisotropy decreases and, in particular, so does its low-energy value $\delta_0 = 3r/2ct$.

As was explained in Sec. 3 for the instantaneous source ($T \ll t$) (the curves 1, 2 in Fig. 3), the restriction, Eq. (5), on the diffusion coefficient is absent and the given results are valid up to $E \approx 1 \cdot 10^{20}$ eV. The diffusion description of the curves 4–6 in Fig. 3 after the break is of progressively worse precision; in fact a transition to quasirectilinear propagation of particles takes place as the anisotropy increases.

As a second candidate for a single source we may take the nearby ($r = 3.5$ Mpc) radiogalaxy Cen A (NGC 5128) with total luminosity $L \approx 1 \cdot 10^{44}$ erg/sec. The calculated spectrum of this source differs little from the spectra given in Figs. 3 and 4, except that for $T \sim t$ the blackbody cutoff is even less noticeable. This source is of interest for the interpretation of the data obtained at Haverah Park²⁵ and Sydney.²⁶ These data show no break in the spectrum up to energies $E \approx 2 \cdot 10^{20}$ eV.

And, lastly, if the time interval between the turning on of the source and the observation is $t \gtrsim 1 \cdot 10^9$ years, then the source may appear at the present time as a normal galaxy. At a distance $r \sim 10$ Mpc the characteristic spectrum and anisotropy will look as in Figs. 3 and 4.

We have compared the calculated spectra with the data obtained at various setups for $E > (0.3-1) \cdot 10^{19}$ eV. We assume that at lower energies the calculated spectrum joins up with the spectrum generated by other sources, for example

galactic or distant metagalactic ones, forming diffuse radiation.

At the present time a contradiction exists between the data of various setups for $E \gtrsim 3 \cdot 10^{19}$ eV. We can describe best with the help of our spectra the measurements of the setups at Haverah Park²⁵ and the "Fly's eye".²⁷ In Fig. 5(a), we show a comparison of the calculations with the data obtained at these setups. Curve 1 corresponds to the model with NGC 4151 as source with $\gamma = 1.1$, $L_p = 2 \cdot 10^{44}$ erg/sec, $t = T = 3 \cdot 10^8$ years, $D_0 = 1 \cdot 10^{35}$ cm²/sec and $\beta = 0.5$. Curves 2 and 3 correspond to the model with Cen A as source with $\gamma = 1.1$, $L_p = 1 \cdot 10^{43}$ erg/sec, $t = T = 3 \cdot 10^8$ years, $D_0 = 3 \cdot 10^{34}$ cm²/sec and $\beta = 0.8$ (curve 2) and $\gamma = 1.1$, $L_p = 1 \cdot 10^{45}$ erg/sec, $t = T = 3 \cdot 10^8$ years, $D_0 = 1 \cdot 10^{35}$ cm²/sec and $\beta = 0.5$ (curve 3). The predicted anisotropy at $E = 1 \cdot 10^{19}$ eV amounts to 25%, 42%, and 19% respectively for the curves 1–3.

In Fig. 5(b), the curves 1 and 2 correspond to the NGC 4151 model with the following parameters: $\gamma = 1.1$, $L_p = 3 \cdot 10^{44}$ erg/sec, $t = 1 \cdot 10^9$ years, $T = 5 \cdot 10^8$ years, $D_0 = 3 \cdot 10^{34}$ cm²/sec and $\beta = 0.5$ (curve 1) and $\gamma = 1.1$, $L_p = 1 \cdot 10^{45}$ erg/sec, $t = 1 \cdot 10^9$ years, $T = 5 \cdot 10^8$ years, $D_0 = 1 \cdot 10^{35}$ cm²/sec and $\beta = 0.5$ (curve 2). The curves 3 and 4 correspond to the Cen A model with the following parameters: $\gamma = 1.3$, $L_p = 7 \cdot 10^{43}$ erg/sec, $t = T = 1 \cdot 10^9$ years, $D_0 = 1 \cdot 10^{35}$ cm²/sec and $\beta = 0.5$ (curve 3) and $\gamma = 1.1$, $L_p = 1.5 \cdot 10^{44}$ erg/sec, $t = 1 \cdot 10^9$ years, $T = 5 \cdot 10^8$ years, $D_0 = 3 \cdot 10^{34}$ cm²/sec and $\beta = 0.5$ (curve 4). The anisotropy for $E = 1 \cdot 10^{19}$ eV amounts to 8.2%, 7.8%, 14% and 2.2% respectively for the curves 1–4.

As can be seen from the figures, we can describe best the spectrum of the "Fly's eye" for $E \gtrsim 1 \cdot 10^{18}$ eV. The predicted

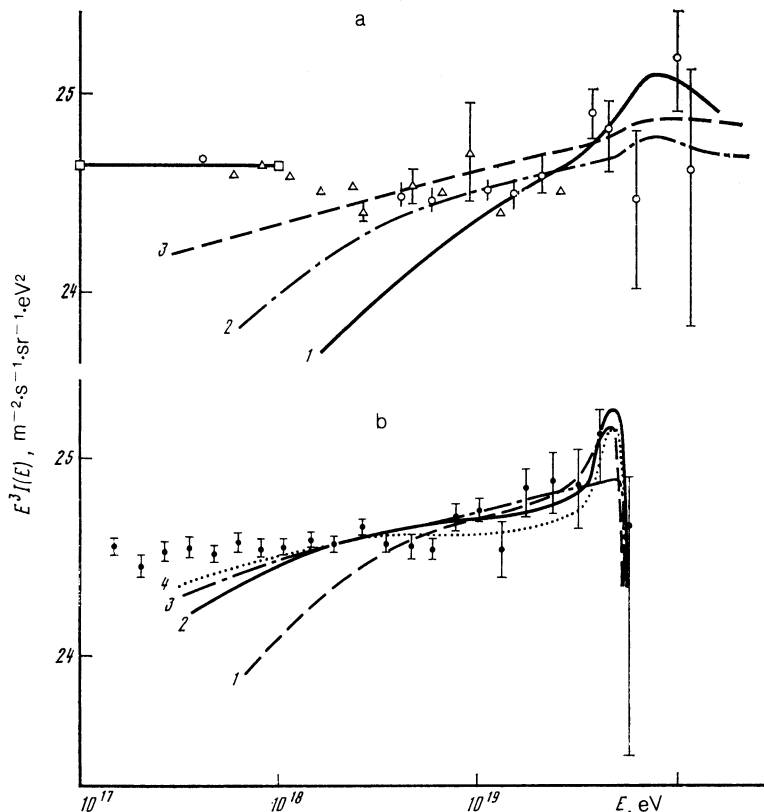


FIG. 5. Comparison of the spectra measured by the setup at Haverah Park²⁵ (a) and "Fly's eye"²⁷ (b) with the spectra of the single-source model. The parameters corresponding to each curve are given in the text.

anisotropy amounts to 2–10% for $E = 1 \cdot 10^{19}$ eV and 2–20% for $E = 5 \cdot 10^{19}$ eV.

7. CONCLUSION

The single-source diffusion models can be naturally divided into two classes: stationary source (stationary diffusion) and pulsed source (nonstationary diffusion). A model of a stationary source, taken to be the Virgo cluster, was discussed in Ref. 2. This model requires very high luminosity $L_p \sim 10^{46}$ erg/sec, which is difficult to ascribe to either one galaxy in the cluster or the total energy output of several active galaxies.

In the case of diffusion models with a single *stationary* source there exist two general restrictions, Eqs. (5) and (6), on the diffusion coefficient. These restrictions show that for a source at a distance of 10–20 Mpc there occurs at an energy of $(5-10) \cdot 10^{19}$ eV a transition to quasirectilinear propagation, characterized by a larger anisotropy. This conclusion applies also to pulsed sources with production pulse duration T of the order of the time of propagation.

Diffusion models with pulsed sources, characterized by $T \ll t$, predict an anisotropy that decreases with increasing energy. As T is increased a general tendency appears for an anisotropy that increases with energy, however at the energy where the spectrum has the photopion bump the anisotropy has a local minimum. The low-energy limit of the anisotropy is in all cases equal to $\delta_0 = 3r/2ct$, where r is the distance from the source and t the time between the turning-on of the source and observation.

The energy spectra are characterized by a late black-body cutoff and a dip at low energies. For large t the black-body cutoff is quite sharp. For $t \sim r^2/D$ and $T \sim t$ the black-body effect on the spectrum can be quite insignificant. Realistic candidates for the single source are NGC 4151, Cen A and NGC 4051. The possibility of an extinguished source also exists.

The main prediction of our models is the relatively low anisotropy ($\sim 10-20\%$ for $E \sim 1 \cdot 10^{19}$ eV) with a direction to the source.

For NGC 4151 for an anisotropy not exceeding 20–30% at an energy of $E \approx 1 \cdot 10^{19}$ eV the spectrum has a black-body cutoff at $E < 10^{20}$ eV and a noticeable photopion hump preceding the cutoff. For a choice of parameters that shift the cutoff energy to higher values the anisotropy increases. For the Cen A source the spectrum may practically have no cutoff at low anisotropy. For an energy E between 10^{18} and

10^{19} eV the calculated spectra should join up with the galactic spectrum or the diffuse metagalactic spectrum.

From among the data obtained at various setups we are able to describe best with the help of our models the spectrum observed at the setup "Fly's eye."

The authors are grateful to V. I. Dokuchaev for useful discussions.

¹¹In the sense of the deviation of Eq. (12), t has the meaning of the time from the turning-on of the source to the moment of detection. Particles emitted after the source was turned on have a propagation time less than t . The shortest propagation time, $t - T$, belongs to particles emitted at the moment when the source was turned off.

¹V. S. Berezinsky and S. I. Grigor'eva, Proc. 16th ICRC (Kyoto) 2, 81 (1979).

²J. Wdowczyk and A. W. Wolfendale, Nature 281, 356 (1979). M. Giler, J. Wdowczyk, and A. W. Wolfendale, J. Phys. G 6, 1561, (1980).

³N. N. Efimov, T. A. Egorov, and A. D. Krasilnikov, Proc. 20th ICRC (Moscow) 2, 41 (1987).

⁴V. S. Berezinskiĭ *et al.*, *Astrophysics of Cosmic Rays* [in Russian] (Nauka, Moscow, 1984).

⁵A. M. Hillas, Ann. Rev. Astron. and Astrophys. 22, 425 (1984).

⁶V. S. Berezinsky and S. I. Grigor'eva, Proc. 15th ICRC (Plovdiv) 2, 309 (1977).

⁷C. T. Hill and D. N. Schramm, Phys. Rev. D 31, 564 (1985).

⁸R. V. E. Lovelace, Nature 262, 649 (1976).

⁹R. D. Blandford, Mon. Not. RAS 176, 465 (1976).

¹⁰R. J. Protheroe and D. Kazanas, Astrophys. J. 265, 620 (1983).

¹¹D. Kazanas and G. E. Ellison, Proc. 19th ICRC (La Jolla) 3, 128 (1985).

¹²T. J. Bogdan and M. G. Webb, Proc. 20th ICRC (Moscow) 2, 195 (1987).

¹³V. S. Berezinsky, Proc. 15th ICRC (Plovdiv) 10, 84 (1977).

¹⁴M. Sikora, J. G. Kirk, M. C. Begelman, and P. Schneider, Astrophys. J. 320, L81 (1987).

¹⁵V. S. Berezinsky and G. T. Zatsepin, preprint #91 P. N. Lebedev Physical Institute, 1971.

¹⁶J. R. Jokipii and G. E. Morfill, Astrophys. J. 290, L1 (1985).

¹⁷H. E. Johnson and W. I. Axford, Astrophys. J. 165, 381 (1971).

¹⁸F. M. Ipavich, Astrophys. J. 196, 107 (1975).

¹⁹I. F. Mirabel and R. Moras, Astrophys. J. 279, 86 (1984).

²⁰C. J. Cesarsky and P. O. Lagage, Proc. 20th ICRC (Moscow) 2, 157 (1987).

²¹R. B. Tully, Astrophys. J. 257, 389 (1982).

²²V. L. Ginzburg and S. I. Syrovatskii, *Origin of Cosmic Rays* [in Russian] (Izd. AN SSSR, Moscow, 1963).

²³V. S. Berezinskiĭ and S. I. Grigor'eva, Zh. Eksp. Teor. Fiz. 93, 812 (1987) [Sov. Phys. JETP 66, 457 (1987)]. V. S. Berezinsky and S. I. Grigor'eva, Astronomy and Astrophysics 199, 1 (1988).

²⁴S. I. Syrovatskii, Astronom. Zh. 36, 17 (1959).

²⁵M. A. Lawrence, R. I. O. Reid, and A. A. Watson, Proc. 20th ICRC (Moscow) 1, 408 (1987).

²⁶M. M. Winn *et al.*, J. Phys. G 12, 653 (1986).

²⁷R. M. Baltrusaitis *et al.*, Proc. 19th ICRC (La Jolla) 2, 146 (1985).

Translated by Adam M. Bincer